

Large climate-induced changes in ultraviolet index and stratosphere-to-troposphere ozone flux

Michaela I. Hegglin* and Theodore G. Shepherd

Now that stratospheric ozone depletion has been controlled by the Montreal Protocol¹, interest has turned to the effects of climate change on the ozone layer^{2,3}. Climate models predict an accelerated stratospheric circulation^{4–6}, leading to changes in the spatial distribution of stratospheric ozone^{2,7} and an increased stratosphere-to-troposphere ozone flux^{8,9}. Here we use an atmospheric chemistry climate model to isolate the effects of climate change from those of ozone depletion and recovery on stratosphere-to-troposphere ozone flux and the clear-sky ultraviolet radiation index—a measure of potential human exposure to ultraviolet radiation. We show that under the Intergovernmental Panel on Climate Change moderate emissions scenario¹⁰, global stratosphere-to-troposphere ozone flux increases by 23% between 1965 and 2095 as a result of climate change. During this time, the clear-sky ultraviolet radiation index decreases by 9% in northern high latitudes—a much larger effect than that of stratospheric ozone recovery—and increases by 4% in the tropics, and by up to 20% in southern high latitudes in late spring and early summer. The latter increase in the ultraviolet index is equivalent to nearly half of that generated by the Antarctic ‘ozone hole’ that was created by anthropogenic halogens. Our results suggest that climate change will alter the tropospheric ozone budget and the ultraviolet index, which would have consequences for tropospheric radiative forcing¹¹, air quality⁸ and human and ecosystem health¹².

Stratospheric ozone depletion from anthropogenic halogens is expected to become negligible by the end of the current century as a result of the Montreal Protocol and its amendments¹. The predicted increase in the stratospheric Brewer–Dobson circulation as a result of climate change^{4–6} acts to decrease ozone in the tropical lower stratosphere and to increase it in the mid-latitude lower stratosphere^{2,7}, especially in the Northern Hemisphere where it leads to a recovery of total ozone to 1960s (that is, pre-ozone-depletion) levels by about 2020 (ref. 2). Although the predicted circulation changes are as yet too small to be seen in measurements^{13,14}, they amount to 15–20% over 50 years⁶. To study the impact of climate change on the ozone layer requires stratosphere-resolving chemistry climate models (CCMs) with interactive stratospheric chemistry^{15,16}. Figure 1 illustrates the predicted circulation and ozone changes between 1960–1970 and 2090–2100 from one such model, the Canadian Middle Atmosphere Model^{17,18} (CMAM). These changes are solely due to climate change, as the abundances of ozone-depleting substances are negligible in both time periods. (As sea surface temperature and the sea-ice distribution are prescribed, there is no long-term memory in the system.) The CMAM was the only model in the SPARC (Stratospheric Processes And their Role in Climate, a project of the World Climate Research Program) CCM Validation intercomparison^{19,20} to provide an ensemble of three simulations

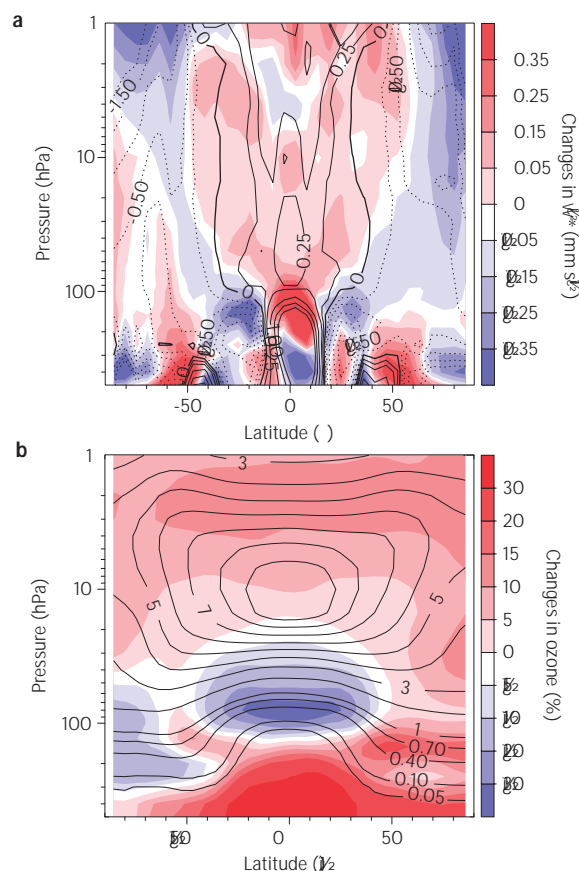


Figure 1 | Predicted changes in the residual vertical velocity and ozone.

a, b, Vertical-latitudinal cross-sections of past values (1960–1970, black contours) and long-term changes (differences between 1960–1970 and 2090–2100, colour shading) for annual mean vertical residual velocity (\bar{w}) (**a**) and ozone (**b**) using an ensemble mean of three simulations from the CMAM. For ozone, the past values are in units of ppmv and the long-term changes are expressed as relative changes.

each extending over 1960–2100 (see the Methods section). Its projections of ozone depletion/recovery and climate change are representative of the average model behaviour¹⁶.

Figure 1a shows the annual mean vertical residual velocity \bar{w} (see the Methods section), which closely approximates vertical transport²¹ and is thus a good indicator of the Brewer–Dobson circulation²². Through an increase in stratospheric wave drag, climate change leads to increased tropical upwelling, particularly in the lower stratosphere⁶. Owing to mass conservation, the rising air masses in the tropics have to be balanced by descending air masses

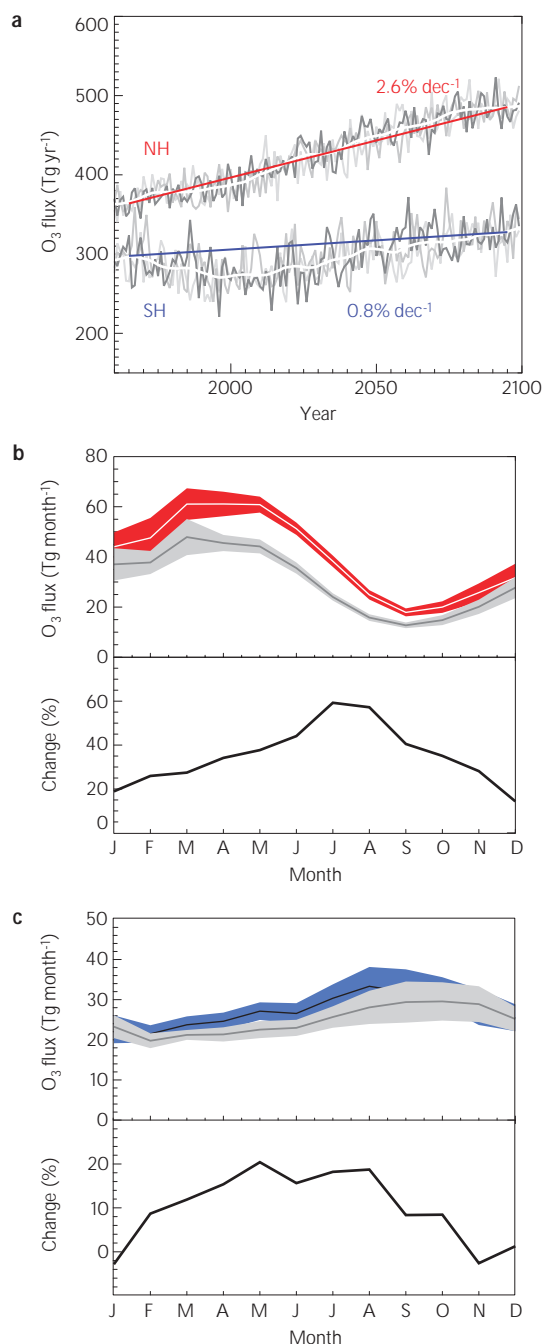


Figure 2 | Predicted changes in STE ozone flux. **a**, Long-term time evolution of annual mean STE ozone flux for both the Northern Hemisphere (NH) and the Southern Hemisphere (SH). Shown are the results of the three CMAM simulations (grey lines), the five-year running ensemble mean (white line) and the long-term trends (between decadal mean values over 1960–1970 and 2090–2100, red and blue lines) excluding the effect of ozone depletion/recovery. **b,c**, Upper panels: monthly mean ozone fluxes 1 s.d. for the Northern Hemisphere (**b**) and Southern Hemisphere (**c**) for the past (1960–1970, grey) and future (2090–2100, red and blue), respectively; lower panels: the relative changes.

in the extratropical lower stratosphere. It is apparent from Fig. 1a that this return flow occurs mainly in the Northern Hemisphere, where it extends to high latitudes. In the Southern Hemisphere, in contrast, the high latitudes show a decrease in downwelling due to a decrease in stratospheric wave drag during Southern Hemisphere spring⁶. The changes in ozone (Fig. 1b) reflect the

Table 1 | Quantified changes in STE ozone flux and ultraviolet index.

(a)	Time period (yr)	O ₃ -flux change (Tg yr ⁻¹)	O ₃ -flux change (%)
Global	1965–2000	1.9 (5.6)	0.3 (0.8)
	2000–2035	60.8 (7.1)	9.2 (1.1)
	1965–2095	151.6 (5.7)	22.9 (0.9)
NH (0° N–90° N)	1965–2000	22.5 (3.7)	6.2 (1.0)
	2000–2035	41.4 (4.2)	10.7 (1.1)
	1965–2095	121.6 (3.7)	33.4 (1.0)
SH (0° S–90° S)	1965–2000	24.4 (5.0)	8.2 (1.7)
	2000–2035	19.4 (5.2)	7.1 (1.9)
	1965–2095	30.0 (5.6)	10.1 (1.9)
(b)	Time period (yr)	UVI change (%)	
Tropics (30° S–30° N)	1965–2000	—	4.7 (0.1)
	2000–2035	—	1.1 (0.1)
	1965–2095	—	3.8 (0.1)
NH (30° N–60° N)	1965–2000	—	3.6 (0.2)
	2000–2035	—	3.9 (0.3)
	1965–2095	—	3.6 (0.2)
NH (>60° N)	1965–2000	—	3.2 (0.5)
	2000–2035	—	6.3 (0.5)
	1965–2095	—	9.1 (0.4)
SH (30° S–60° S)	1965–2000	—	7.4 (0.4)
	2000–2035	—	3.6 (0.4)
	1965–2095	—	0.0 (0.4)
SH (>60° S)	1965–2000	—	21.0 (1.0)
	2000–2035	—	8.7 (1.4)
	1965–2095	—	3.2 (1.0)
SH (>60° S, OND)	1965–2000	—	37.2 (2.9)
	2000–2035	—	13.2 (3.4)
	1965–2095	—	10.2 (2.0)

Shown are global, Northern Hemisphere (NH), Southern Hemisphere (SH) and/or Tropics absolute and/or relative change in STE ozone flux (**a**) and ultraviolet index (UVI) (**b**) for different time periods encompassing ozone depletion (1965–2000), initial ozone recovery (2000–2035) and climate change (1965–2095). Polar night is excluded from the UVI averages. For 2000–2035, UVI % changes are expressed in units of change relative to the 1965 baseline, to be consistent with Fig. 3c. Time differences are estimated on the basis of 10-year averages around each endpoint. Uncertainties represent standard errors of the differences. OND: October, November, December.

changes in w . Ozone decreases in a shallow layer just above the tropical tropopause, and increases in a shallow layer just below 100 hPa (approximately 16 km) in mid-latitudes. In the Northern Hemisphere this increase extends all the way to the pole, but in the Southern Hemisphere it is restricted to mid-latitudes, the high latitudes showing instead a decrease in lower stratospheric ozone resulting from the decreased downwelling in Southern Hemisphere spring. There is a widespread increase in ozone in the upper stratosphere owing to climate-change-induced cooling²³, but this has only a small impact on total ozone². Tropospheric increases of up to 30% are seen, but given the lack of tropospheric chemistry in the CMAM (see the Methods section) they should not be seen as a realistic projection.

The accelerated Brewer–Dobson circulation and its effects on the ozone distribution can be expected to lead to an increase in stratosphere-to-troposphere (STE) ozone flux. A recent study⁸ compared the projections of 10 tropospheric CCMs used for the Intergovernmental Panel on Climate Change (IPCC) fourth assessment report⁹ (AR4) and found that the STE ozone flux

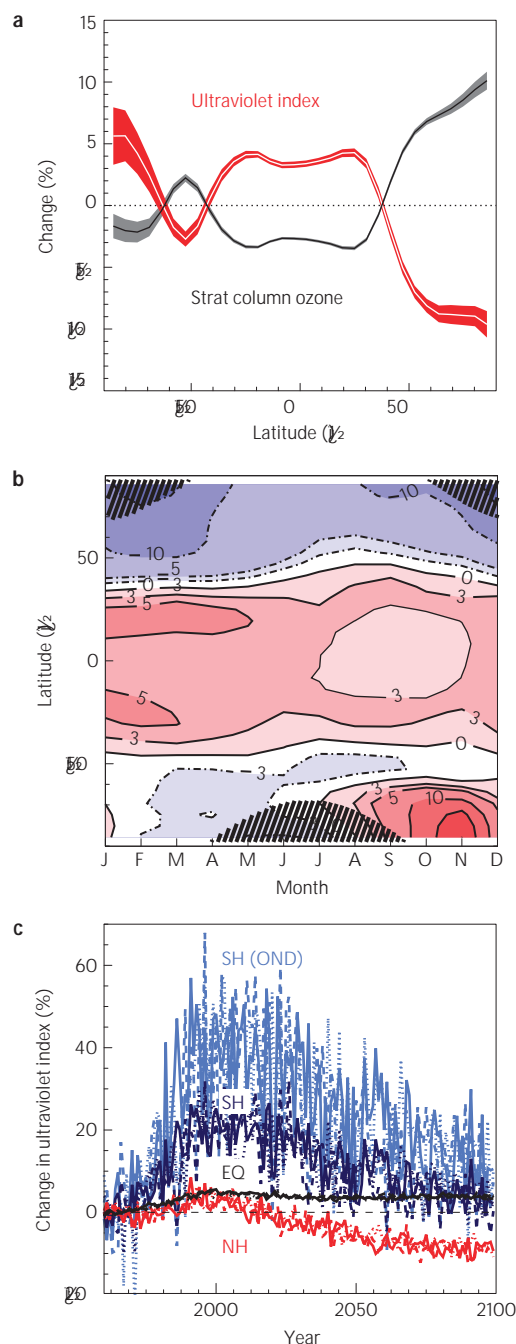


Figure 3 | Predicted changes in ultraviolet index. **a**, Relative change between 1960–1970 and 2090–2100 in annual mean stratospheric column ozone (black line), with the 2 PVU tropopause as the lower boundary, and annual mean relative change in ultraviolet index (white line) excluding polar night. Shadings represent standard errors of the mean. **b**, Latitudinal-seasonal dependence of relative change in ultraviolet index between 1960–1970 and 2090–2100. Polar night is indicated by black hatching. **c**, Time evolution of the ultraviolet index changes for 30°S–30°N (EQ, black), 60°N–90°N (NH, red), 60°S–90°S (SH, dark blue) and 60°S–90°S, but only for October–December (SH (OND), light blue). The different line styles indicate the three simulations.

increased as a result of climate change in almost all of the models. However, these models generally do not resolve the stratospheric circulation and constrain stratospheric ozone by relaxing to a prescribed value^{8,9}. The latter procedure introduces artificial sources or sinks of ozone, which is problematical

when looking at long-term changes, and does not represent the effects of changes in stratospheric ozone from climate change or ozone depletion/recovery. Here we use the CMAM to provide the first quantification of the increased STE ozone flux using a stratosphere-resolving, fully interactive (hence, self-consistent) CCM, isolating the effects of climate change from those of ozone depletion/recovery. We quantify the STE ozone flux using a simple box-model approach (see the Methods section).

Global STE ozone flux in the CMAM averaged over 1995–2005 is 655 ± 5 (standard error) Tg yr^{-1} . This value lies within the (rather uncertain) observational range⁹ of $540 \pm 140 \text{ Tg yr}^{-1}$, as well as within the tropospheric model range⁸ of $550 \pm 170 \text{ Tg yr}^{-1}$. Figure 2a shows the time evolution of annual mean STE ozone flux over 1960–2100. Both hemispheres show an increase across the entire time period (indicated with the straight line connecting past and future values), which can be attributed to climate change. The increase is modulated by ozone depletion, which maximizes around 2000, and ozone recovery, which is predicted to occur before the end of the current century, in accord with the rise and fall of the abundance of ozone-depleting substances¹⁶. The impact of climate change is much stronger in the Northern Hemisphere than in the Southern Hemisphere, whereas that of ozone depletion is much stronger in the Southern Hemisphere than in the Northern Hemisphere. The dominance of the ozone-depletion signal in the Southern Hemisphere is such that STE ozone flux is predicted to have decreased over the past few decades and will return to 1960s values only in the middle of the current century. In contrast, STE ozone flux in the Northern Hemisphere is predicted to increase steadily through the entire record, with the most rapid increase occurring over the next few decades when ozone recovery and the strengthening Brewer–Dobson circulation act in concert. The results are quantified in Table 1 for the three periods 1965–2000 (encompassing ozone depletion), 2000–2035 (encompassing initial ozone recovery) and 1965–2095 (the long-term changes, which are attributable entirely to climate change). The increase in global STE ozone flux over the slightly shorter time period 2000–2030 is 50 ± 6 (standard error) Tg yr^{-1} , which is near the middle of the tropospheric model range⁸ of $41 \pm 31 \text{ s.d.} \text{ Tg yr}^{-1}$.

Figure 2b,c shows the seasonal cycle of STE ozone flux for the past and future in each hemisphere, together with the relative changes. Note the different vertical ranges for the two hemispheres. The seasonal cycle maximizes in spring and is stronger in the Northern Hemisphere than in the Southern Hemisphere, as found in other studies²⁴. In the Northern Hemisphere, STE ozone flux increases as a result of climate change in all months, with the largest absolute increases in spring and the largest relative increases in summer, where they reach 60%. In the Southern Hemisphere, the increases are comparatively modest and maximize in winter.

The effect of climate change on stratospheric ozone seen in Fig. 1b is summarized in terms of its impact on stratospheric column ozone in Fig. 3a. The global mean change is close to zero, but there are pronounced changes over particular latitude ranges, which point to the role of transport². There are increases of 5–10% in the Northern Hemisphere at latitudes higher than 45° and decreases of roughly 3% in the tropics and 2% at southern high latitudes. These changes have implications for the ultraviolet radiation reaching the Earth's surface, which are quantified here.

A simple approximate formula relating stratospheric column ozone to the ultraviolet index (UVI, an accepted measure of potential human exposure to solar ultraviolet radiation²⁵) under cloud-free, unpolluted, low-surface-albedo conditions is given by

$$\text{UVI} = 12.5 \cdot \cos^{2.42} \theta \cdot \left(\frac{\text{DO}}{300} \right)^{1.23}$$

where $\cos \theta$ is the cosine of the solar zenith angle and DO is in Dobson

units²⁵. Sufficiently small changes in UVI and Δ are then related by

$$\frac{\Delta \text{UVI}}{\text{UVI}} = 1.23 \frac{\Delta}{\text{UVI}}$$

showing that the relative changes are linearly related (for a given solar zenith angle). We use this latter relation to translate relative changes in stratospheric column ozone to relative changes in ultraviolet index, on a monthly mean basis.

Figure 3a shows the annual mean of these relative changes in ultraviolet index (excluding polar night) between 1960–1970 and 2090–2100, to isolate the impact of climate change. Ultraviolet index is seen to increase by about 4% in the tropics and by 3–6% in southern high latitudes. In the Northern Hemisphere, the transport-induced increase in ozone leads to a decrease in ultraviolet index by 9% at high latitudes. Figure 3b shows the relative changes in ultraviolet index as a function of latitude and month. The tropical increase and the Northern Hemisphere decrease are fairly uniform over the year, whereas in southern high latitudes there is a pronounced maximum in the ultraviolet index change during spring and early summer. Figure 3c shows the time evolution of the ultraviolet index changes. In all regions, ultraviolet index increases up to about 2000 and then decreases in the future, with these changes largely driven by ozone depletion and recovery²⁶. However, the changes between 1960–1970 and 2090–2100 isolate the effects of climate change, which as argued above are mainly of dynamical origin. Table 1 quantifies the relative changes in ultraviolet index for the same time periods as for STE ozone flux for various latitude bands. In the Northern Hemisphere and the tropics, the long-term changes are comparable in magnitude to the effects of ozone depletion (although of opposite sign in the Northern Hemisphere); in fact for 60°N–90°N the effects of climate change are three times as large as those of ozone depletion.

The Southern Hemisphere high latitudes over October–December show not only the largest long-term changes, due to both ozone depletion and climate change, but also the largest interannual variability. Thus, for this region and season it is important to consider not just the multi-year means but also the extreme values of the ultraviolet index. From Fig. 3c it is seen that climate change leads to an increase in the seasonally averaged ultraviolet index of up to 20%, which is nearly one-half the maximum values of about 50% arising from the effect of the ozone hole.

The strength and novelty of our study comes from its use of a stratospheric CCM run over long timescales, which allows the identification of the effects of climate change and their separation from (and comparison with) the effects of ozone depletion and recovery. The use of a stratospheric CCM for the quantification of changes in STE ozone flux and (clear-sky) ultraviolet index is justifiable, because these quantities are controlled by stratospheric circulation and the distribution of stratospheric ozone. However, to assess the impact of these changes on tropospheric chemistry, the tropospheric ozone budget and air quality, a future generation of CCMs will be required that includes both stratospheric and tropospheric chemistry. In addition, the amount of ultraviolet radiation actually reaching the Earth's surface is controlled by various tropospheric factors, such as aerosols and cloudiness, which may change under climate change, although these changes are considered very uncertain¹. Nevertheless, our study shows the need to account for the effect of climate change, not just ozone depletion and recovery, on stratospheric ozone when predicting future changes in tropospheric chemistry and ultraviolet radiation, for example, in future IPCC assessments or studies of ecosystem (for example, phytoplankton, crop productivity) and human health (for example, vitamin D production) responses to ozone changes. Our study also highlights the need to monitor the development of the ozone layer quite apart from its recovery from halogen-induced

ozone depletion, to see whether the predictions of an accelerated Brewer–Dobson circulation and associated changes in ozone are confirmed in observations.

Methods

Model description. The CMAM is the upward extension of the Canadian Centre for Climate Modelling and Analysis third generation general circulation model¹⁸ (CCCma-AGCM3). The climate sensitivity of the latter's coupled atmosphere–ocean model version (CGCM3.1), which is defined as the equilibrium global mean surface temperature change following a doubling of atmospheric CO₂ concentration, is 3.4 °C (ref. 27). This corresponds roughly to the average climate sensitivity of 3.2 °C found among the AR4 models²⁷. The CMAM includes a comprehensive stratospheric chemistry, radiation scheme and representation of the relevant physical processes in a fully interactive mode¹⁷. Chemistry is calculated down to around only 400 hPa. Chemical tracers transported below this level are still advected and mixed by the atmosphere, but are chemically inert. A constant dry deposition velocity is prescribed that removes certain tracers when they mix to the ground (including ozone and HCl). The ozone found in the troposphere therefore results mostly from transport. Model fields are calculated on a linear Gaussian transform grid with 32–64 grid points in the horizontal, corresponding to a spatial resolution of around 6–6 and 71 vertical levels, reaching from the ground up to around 100 km altitude. The vertical resolution in the tropopause region is around 900 m, coarsening to around 2 km in the upper stratosphere. For the calculations presented in this study, we use monthly mean fields of an ensemble of three 150-year transient runs from 1950, carried out as part of the SPARC CCM Validation Intercomparison¹⁶. Greenhouse-gas surface concentrations evolve in time following scenario A1B (medium) of the IPCC Special Report on Emission Scenarios¹⁰. The surface halogens are prescribed according to the Ab scenario given by the World Meteorological Organization²⁸. No further external forcing (for example, from solar variability or volcanoes) is prescribed. The three ensemble members are forced by independent realizations of sea surface temperatures and sea-ice distributions from IPCC AR4 simulations with CGCM3.1 under the A1B scenario.

Calculation of the STE ozone flux. We quantify the STE ozone flux in each hemisphere on a monthly mean basis using a simple box-model approach previously used for mass flux calculations²⁹ (see Supplementary Fig. S1), but applied instead to ozone:

$$F_{\text{out}} \approx F_{\text{in}} - \frac{dM}{dt}$$

Here F_{in} is the downward flux of ozone across the 100 hPa surface, estimated as the area-weighted integral within each hemisphere of the zonal and monthly mean ozone concentration multiplied by the negative of the monthly mean residual vertical velocity w at every latitude gridpoint, where w is calculated as in ref. 6, and M is the total mass of ozone contained in the lowermost stratosphere (defined as the region between the 100 hPa surface and the 2 PVU (potential vorticity unit, with 1 PVU $\equiv 10^{-6} \text{ K m}^2 \text{ kg}^{-1} \text{ s}^{-1}$) dynamical tropopause). The STE ozone flux, F_{out} , is then calculated as a residual. In this diagnostic we do not account for chemical sources and sinks of ozone in the lowermost stratosphere, because the photochemical lifetime of ozone is much greater than its residence time in this region³⁰. The term dM/dt accounts for the 'seasonal breathing' of the lowermost stratosphere, and leads to a time lag between F_{in} and F_{out} . F_{in} maximizes in mid-winter, at the peak of the Brewer–Dobson circulation; dM/dt also maximizes in mid-winter; F_{out} maximizes in late spring/early summer. Supplementary Fig. S2 shows the seasonal dependence of these three components averaged over 1995–2005 for each hemisphere. (The curves in Supplementary Fig. S2c are similar to the grey curves in Fig. 2b,c, which are averaged over 1960–1970.) The seasonal cycle of STE ozone flux is much more pronounced in the Northern Hemisphere than in the Southern Hemisphere, because of the much stronger Brewer–Dobson circulation in the Northern Hemisphere²².

Received 10 March 2009; accepted 10 July 2009; published online 6 September 2009

References

- World Meteorological Organization. *Scientific Assessment of Ozone Depletion: 2006*, WMO/U.N. Environ. Prog. Rep. 50 (WMO, 2007).
- Shepherd, T. G. Dynamics, stratospheric ozone, and climate change. *Atmos. Ocean* **46**, 117–138 (2008).
- Waugh, D. W. *et al.* Impacts of climate change on stratospheric ozone recovery. *Geophys. Res. Lett.* **36**, L03805 (2009).
- Butchart, N. & Scaife, A. A. Removal of chlorofluorocarbons by increased mass exchange between the stratosphere and troposphere in a changing climate. *Nature* **410**, 799–802 (2001).
- Butchart, N. *et al.* Simulations of anthropogenic change in the strength of the Brewer–Dobson circulation. *Clim. Dyn.* **27**, 727–741 (2006).

6. McLandress, C. & Shepherd, T. G. Simulated anthropogenic changes in the Brewer–Dobson circulation, including its extension to high latitudes. *J. Clim.* **22**, 1516–1540 (2009).
7. Li, F., Stolarski, R. S. & Newman, P. A. Stratospheric ozone in the post-CFC era. *Atmos. Chem. Phys.* **9**, 2207–2213 (2009).
8. Stevenson, D. S. *et al.* Multimodel ensemble simulations of present-day and near-future tropospheric ozone. *J. Geophys. Res.* **111**, D8301 (2006).
9. Denman, K. L. *et al.* in *IPCC Climate Change 2007: The Physical Science Basis* (eds Solomon, S. *et al.*) (Cambridge Univ. Press, 2007).
10. Intergovernmental Panel on Climate Change. *Special Report on Emissions Scenarios: A Special Report of Working Group III of the Intergovernmental Panel on Climate Change* (Cambridge Univ. Press, 2000).
11. Forster, P. & Shine, K. Radiative forcing and temperature trends from stratospheric ozone changes. *J. Geophys. Res.* **102**, 10841–10855 (1997).
12. United Nations Environment Program. *Environmental Effects of Ozone Depletion and its Interactions with Climate Change: 2006 Assessment* ISBN: 978-92-807-2821-7 (UNEP, 2006).
13. Waugh, D. W. The age of stratospheric air. *Nature Geosci.* **2**, 14–16 (2009).
14. Engel, A. *et al.* Age of stratospheric air unchanged within uncertainties over the past 30 years. *Nature Geosci.* **2**, 28–31 (2009).
15. Austin, J. *et al.* Uncertainties and assessments of chemistry-climate models of the stratosphere. *Atmos. Chem. Phys.* **3**, 1–27 (2003).
16. Eyring, V. *et al.* Multimodel projections of stratospheric ozone in the 21st century. *J. Geophys. Res.* **112**, D16303 (2007).
17. de Grandpré, J. *et al.* Ozone climatology using interactive chemistry: Results from the Canadian middle atmosphere model. *J. Geophys. Res.* **105**, 26475–26491 (2000).
18. Scinocca, J., McFarlane, N. A., Lazare, M., Li, J. & Plummer, D. Technical Note: The CCCma third generation AGCM and its extension into the middle atmosphere. *Atmos. Chem. Phys.* **8**, 7055–7074 (2008).
19. Eyring, V. *et al.* Assessment of temperature, trace species, and ozone in chemistry-climate model simulations of the recent past. *J. Geophys. Res.* **111**, D22308 (2006).
20. Waugh, D. W. & Eyring, V. Quantitative performance metrics for stratospheric-resolving chemistry-climate models. *Atmos. Chem. Phys.* **8**, 5699–5713 (2008).
21. Andrews, D. G., Holton, J. R. & Leovy, C. B. *Middle Atmosphere Dynamics* (Academic, 1987).
22. Shepherd, T. G. Transport in the middle atmosphere. *J. Meteorol. Soc. Japan* **85B**, 165–191 (2007).
23. Jonsson, A. I., de Grandpré, J., Fomichev, V. I., McConnell, J. C. & Beagley, S. R. Doubled CO₂-induced cooling in the middle atmosphere: Photochemical analysis of the ozone radiative feedback. *J. Geophys. Res.* **109**, D24103 (2004).
24. Hsu, J., Prather, M. J. & Wild, O. Diagnosing the stratosphere-to-troposphere flux of ozone in a chemistry transport model. *J. Geophys. Res.* **110**, D19305 (2005).
25. Madronich, S. Analytic formula for the clear-sky UV index. *Photochem. Photobiol.* **83**, 1537–1538 (2007).
26. Tourpali, K. *et al.* Clear sky UV simulations in the 21st century based on ozone and temperature projections from chemistry-climate models. *Atmos. Chem. Phys.* **9**, 1165–1172 (2009).
27. Randall, D. A. *et al.* in *IPCC Climate Change 2007: The Physical Science Basis* (eds Solomon, S. *et al.*) (Cambridge Univ. Press, 2007).
28. World Meteorological Organization. *Scientific Assessment of Ozone Depletion: 2002, Global Ozone Research and Monitoring Project Rep.* 47 (WMO, 2003).
29. Appenzeller, C., Holton, J. & Rosenlof, K. Seasonal variation of mass transport across the tropopause. *J. Geophys. Res.* **101**, 15071–15078 (1996).
30. Olsen, M. A., Schoeberl, M. R. & Douglass, A. R. Stratosphere–troposphere exchange of mass and ozone. *J. Geophys. Res.* **109**, D24114 (2004).

Acknowledgements

The authors would like to acknowledge helpful discussions with V. Fioletov on ultraviolet index and C. McLandress on STE ozone fluxes. This study has been financially supported by the Canadian Foundation for Climate and Atmospheric Sciences (CFCAS) through the C-SPARC project, which provided the CMAM simulations.

Author contributions

M.I.H. initiated the project and analysed the model data. T.G.S. helped in the data interpretation and with the writing of the manuscript.

Additional information

Supplementary information accompanies this paper on www.nature.com/naturegeoscience. Reprints and permissions information is available online at <http://npg.nature.com/reprintsandpermissions>. Correspondence and requests for materials should be addressed to M.I.H.